Poly(2-amino-8-methyladenylic acid). Competing Structural and Energetic Effects of Substituents

Frank B. Howard,* Wongil Limn, and H. Todd Miles*
Laboratory of Molecular Biology, National Institute of Arthritis, Diabetes, and Digestive and Kidney Diseases, National Institutes of Health, Bethesda, Maryland 20205
Received February 15, 1985

ABSTRACT: The ribopolynucleotide poly(2-amino-8-methyladenylic acid), $(r2NH_28MeA)_n$, has been synthesized, and its physical and chemical properties have been examined. The study reveals competing effects on these properties of the 2-NH_2 and 8-Me substituents. In marked contrast to the analogous $(r8MeA)_n$, the new polymer readily interacts to form double helixes with complementary pyrimidine polynucleotides. Triple helixes are not formed. The 8-Me group is strongly destabilizing for helix formation ($\Delta T_m \sim 65$ °C), presumably by favoring a syn conformation, which blocks heteroduplex formation with ribohomopolymers. The 2-NH_2 substituent stabilizes helixes in the ribo series by about 30 °C in T_m by forming a third interbase hydrogen bond. We suggest that the free energy from the 2-NH_2 interaction drives the syn–anti equilibrium to the purine polymer to the anti form present in the double helix. CD spectra of the homopolymers $(r2NH_2A)_n$ and $(r2NH_28MeA)_n$ are completely different, reflecting major differences of conformation. The double helixes formed by these polymers with $(rT)_n$ and $(rBrU)_n$, on the other hand, have closely similar CD spectra, supporting our proposal of a major change in conformation of $(2NH_28MeA)_n$ on going from single strand to double helix.

Purine nucleotides and polynucleotides can exist in both syn and anti conformations and are interconverted by rotation of the base about the glycosidic bond. The anti form is predominant, but the rotational barrier is relatively low. The importance of the syn form has been emphasized in recent years by the discovery of Z DNA (Wang et al., 1979; Drew et al., 1980) in which all of the purine residues are syn. The B to Z transition is favored by a number of factors, including high salt, ethanol, chemical substitution, ligand binding, and incorporation in supercoiled, closed-circular DNA. The reasons for the effectiveness of these factors are in most cases not clear, though presumably 8-position substituents of G contribute to the Z form by favoring the syn conformation (see below). The presence of Z DNA in chromosomes has been indicated by specific antibody probes, and a regulatory role has been suggested for Z-form regions [for a recent review of Z DNA, see Zimmerman (1982)]. A possible biological function of the syn conformation in non-Z structures has also been suggested for the A residues in messenger RNAs which bind to the initial I in some anticodons (Sakore & Sobell, 1969). The syn conformation would have the advantage in this and other cases of purine–purine pairing of providing the same C1′–C1′ distance as the purine–pyrimidine pairs present in the same chain.

It is important to understand better the factors which affect and may be used to control the syn–anti equilibrium in both natural and synthetic nucleic acids. One of the most useful methods for this purpose is the introduction of bulky substituents at C8, known to alter the equilibrium and favor the syn form [cf. Ikehara et al. (1969), Michelson et al. (1970), Tavale & Sobell (1970), Howard et al. (1974, 1975), and Govil et al. (1981)]. Thus, for example, $(r8BrA)_n$ forms a highly stable double-helical self-structure but fails to interact with $(rU)_n$ or $(rBrU)_n$. All residues are in the syn form (Howard et al., 1974, 1975; Govil et al., 1977, 1981), and the bases are mutually hydrogen bonded at N1 and N6. $(rA)_n$, on the other hand, has a partially stacked single-stranded structure of relatively low stability (Leng & Felsenfeld, 1966; Applequist & Damle, 1966; Brahms, 1965; Holcomb & Tinoco, 1965; Eisenberg & Felsenfeld, 1967). The 8-methyl substituent is similar to 8-Br in size but less perturbing electronically. In a series of dimers of adenylic acid partially or completely substituted with 8-Me, the 8-MeA residues appeared to have either syn or anti conformations (Uesugi et al., 1978; Ikehara et al., 1978). Major structural effects on a polynucleotide of perturbing the syn–anti equilibrium are indicated by a study of poly(8MeA) (Limn et al., 1983). This polymer differs from both $(rA)_n$ and $(r8BrA)_n$ in forming a regular single-stranded helix in neutral solution rather than a nonregular or a double-stranded helix. $(r8MeA)_n$ does not react with $(rU)_n$ or $(rBrU)_n$ and has NMR properties consistent with a regularly alternating syn and anti arrangement of the bases.

In the present study, we retain the 8-Me substitution but modulate its effects by also introducing a NH_2 group in the 2-position. The 2-NH_2 group in poly(A) and its derivatives is known to form three hydrogen bonds to U and T, increasing the stability of the helixes that are formed (Howard et al., 1966, 1976; Muraoka et al., 1980). We find that $(2NH_28MeA)_n$, unlike $(8MeA)_n$, forms complexes with all of the complementary pyrimidine polynucleotides examined. The third hydrogen bond to U and T formed by the 2-amino group appears to supply the free energy to drive the conformational equilibrium of the purine polymer to the anti form, permitting helix formation with complementary pyrimidine polymers.

The structure of the repeating unit of this polymer, $2NH_28Me5'AMP$, has been determined by X-ray crystallography (Silverton et al., 1982). In the crystal, the nucleotide molecules adopt the unusual syn-C4′-exo conformation and are arranged in triangular groupings with phosphate groups in the center and bases on the periphery. Extensive hydrogen bonding and water bridges control molecular association.

Materials and Methods

2-Amino-8-methyladenosine 5′-Diphosphate. The monophosphate (370 mg; Limn et al., 1982) was converted to the diphosphate by the general procedure of Moffat & Khorana (1961). The diphosphate was obtained in 80% yield after elution from a DEAE-Sephadex A25 column (2.4 × 30 cm)

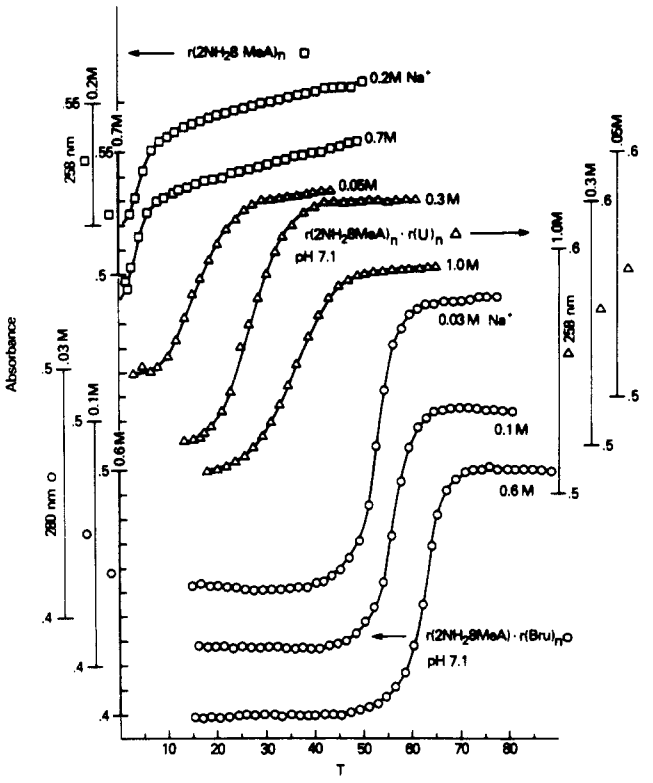

FIGURE 1: UV melting curves of $(r2NH_28MeA)_n$ [(□) upper left scales] at $[Na^+]$ = 0.2 and 0.7 M, 0.002 M sodium pyrophosphate, pH 8, of $(r2NH_28MeA)_n \cdot (rU)_n$ [(△) right scales] at $[Na^+]$ = 0.05, 0.3, and 1 *M*, 0.002 M sodium phosphate, pH 7.1, and of $(r2NH_28MeA)_n \cdot (rBrU)_n$ [(○) lower left scales] at $[Na^+]$ = 0.03, 0.1, and 0.6 M, 0.008 M sodium phosphate, pH 7.1; [total polymer P] = 6×10^{-5} M for all three polymer systems.

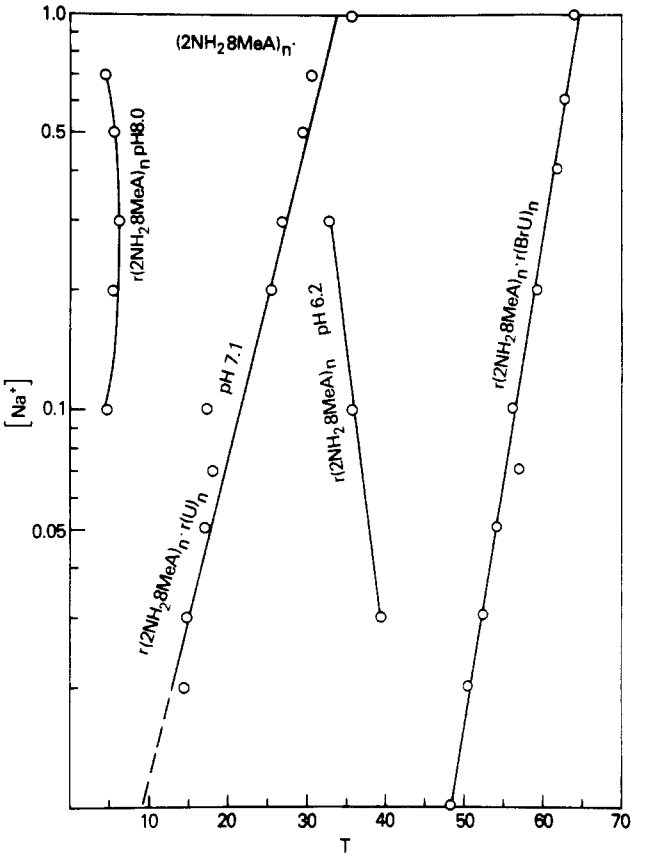

FIGURE 2: Dependence of T_m upon $[Na^+]$ of self-interacted $(r2NH_28MeA)_n$ in 0.002 M sodium pyrophosphate, pH 8.0 (left) and 6.2 (center), of $(r2NH_28MeA)_n \cdot (rU)_n$ in 0.002 M sodium phosphate, pH 7.1, and of $(r2NH_28MeA)_n \cdot (rBrU)_n$ in 0.008 M sodium phosphate, pH 7.1.

with a linear gradient of triethylammonium bicarbonate buffer.

Poly(2-amino-8-methyladenylic acid). The diphosphate was polymerized with polynucleotide phosphorylase from *Micrococcus luteus* (type 15, P-L Biochemicals). The reaction mixture contained 0.013 M substrate, 0.015 M $MgCl_2$, 0.1 M tris(hydroxyethyl)aminomethane (Tris) buffer (pH 9.0), 2×10^{-4} M ethylenediaminetetraacetic acid (EDTA), 1×10^{-4} M dithiothreitol, and 50 units of polynucleotide phosphorylase in a total volume of 12 mL; 36% of the substrate was polymerized in 1.5 days at 38 °C as determined by release of inorganic phosphate. Protein was removed by phenol extraction. The polymer was dialyzed in turn against the following solutions: 2 L of 0.5 M NaCl–0.001 M EDTA (pH 8.04), 4 L of 0.5 M NaCl, 4 L of 0.3 M NaCl, 4 L of 0.1 M NaCl, and 4 L of distilled water. This solution was lyophilized to yield 43 mg of polymer.

Mixing curves were determined by a procedure which we have described (Howard et al., 1971, 1976), a separate solution being prepared for each composition. A Cary Model 118 spectrophotometer was used for UV spectral measurements. The spectrophotometer was interfaced to an LDACS computer system (Powell et al., 1980). Data were analyzed with a Digital Equipment Corp. Model 11/70 computer by the method described previously (Howard et al., 1976).

Melting curves were measured automatically with either a Cary Model 118 or a Model 210 spectrophotometer, the spectrophotometers and accessory equipment operating in a closed-loop mode with the LDACS computer system (Howard et al., 1977).

CD spectra were measured with a Jasco J-500A spectrophotometer, also interfaced to the LDACS system.

The molar extinction coefficient of $(r2NH_28MeA)_n$ was determined by analysis for phosphorus as described previously (Muraoka et al., 1980) with a 5-fold reduction in scale. The mean of five determinations was 9660 with a standard deviation of 140 (0.002 M sodium pyrophosphate, pH 8.0; 0.1 M Na^+).

Electrophoresis of $(r2NH_28MeA)_n$ end-labeled with ^{32}P (Maxam & Gilbert, 1980) on a 20% polyacrylamide gel in 0.1 M Tris–borate buffer, pH 8.3, and 4 mM EDTA for 4.7 h at 1500 V and 11 mA revealed a polydisperse polymer, most of which (about 80%) migrated between marker bands of 310 and 603 base pairs (ϕX174 RF DNA–*Hae*III digest, New England Biolabs).

RESULTS

Homopolymer at pH 8. At $[Na^+]$ = 0.1 M and higher, the homopolymer exhibits a sharp ($\sigma \simeq 5$ °C) transition at low temperature, with an absorbance increase of ~15% at 257 nm (Figure 1). Above 20 °C, the absorbance increases linearly with temperature (Figure 1). T_m is almost independent of $[Na^+]$ (Figure 2). Below 0.1 M Na^+, only the beginning of a transition can be detected.

Homopolymer in Acid Solution. At pH 6.2, the homopolymer has a broad but cooperative melting curve with T_m = 35.7 °C and σ = 18 °C in 0.1 M Na^+. The salt dependence curve has a $dT_m/d \log [Na^+]$ value of –6.5 °C (Figure 2). The absorbance at 280 nm increases by 46% from the bottom to the top of the main transition in 0.03 M Na^+ and by 55% in 0.1 and 0.3 M Na^+.

Interaction with $(rT)_n$ and $(rBrU)_n$: Stoichiometry. A method of analyzing UV, CD, or other characteristic spectra to establish the combining ratio of interacting polynucleotides

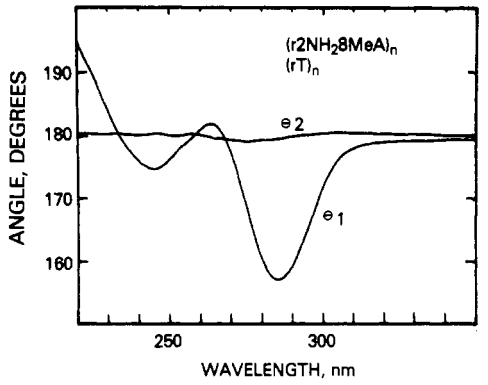

FIGURE 3: Dependence on wavelength of angles of intersection of CD mixing curves corresponding to 50% $(rT)_n$ (θ_1) and 67% $(rT)_n$ (θ_2) in the $(r2NH_28MeA)_m$, $(rT)_n$ system. The most favorable wavelength for detecting the 1:1 complex occurs at 286 nm (θ_1). θ_2 is approximately 180° over the range 220–350 nm, indicating that a 1:2 complex is not formed. Conditions: 0.002 M sodium pyrophosphate, pH 8.0; 0.1 M Na^+; [total polymer P] = 8×10^{-5} M; 10 °C.

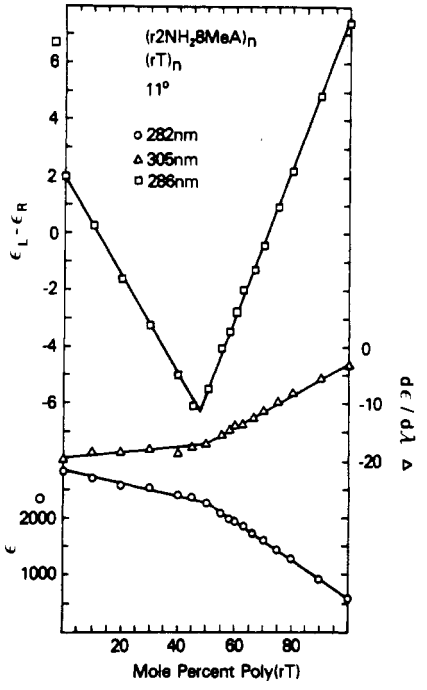

FIGURE 4: Mixing curves. UV [(O) lower left scale], derivative UV [(Δ) right scale], and CD [(□) upper left scale] mixing curves plotted at three wavelengths have clear breaks at the 1:1 ratio, demonstrating formation of $(r2NH_28MeA)_n{\cdot}(rT)_n$. Conditions are those of Figure 3.

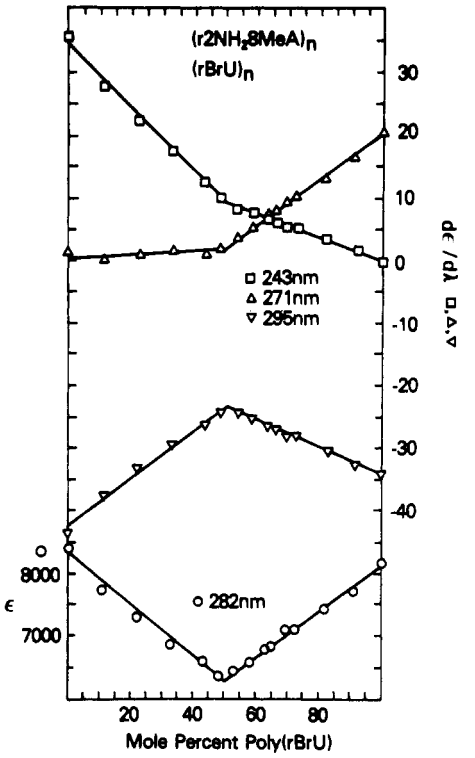

FIGURE 5: Mixing curves for the interaction of $(r2NH_28MeA)_n$ and $(rBrU)_n$. UV (O), lower left scale; derivative UV, all other curves, right scale.

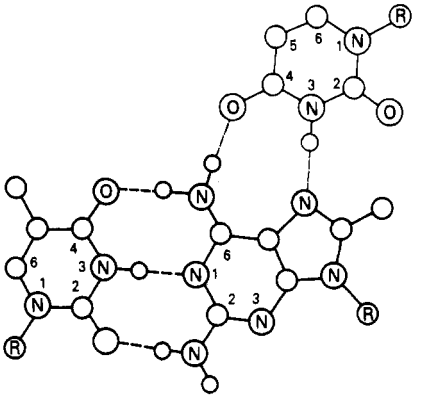

FIGURE 6: Hydrogen bonding scheme of double helix formed by $(r2NH_28MeA)_n$ and $(rT)_n$ (heavier lines). A second pyrimidine strand (lighter lines, upper right) would need to occupy the position shown in order to form hydrogen bonds. The close contact between 8-Me and 2-O, in fact, prevents attachment of a third strand (see text).

has been described previously (Howard et al., 1976, 1977) and is applied here to complexes of $(2NH_28MeA)_n$. Angles of intersection of mixing curves at relevant mole fractions (usually 0.5 and 0.67) are defined as dependent variables, θ_1 and θ_2, which are calculated by computer as continuous functions of wavelength, as in Figure 3. Maxima and minima in these dispersion curves correspond to optimum wavelengths for mixing curves. When $\theta_i = 180°$ over the entire spectrum, there is no break in the mixing curve at any wavelength, and a complex corresponding to X_i is not formed. In the dispersion curve calculated from CD spectra of mixtures of $(r2NH_2A)_n$ and $(rT)_n$, θ_1 has its greatest magnitude at 286 nm (Figure 3), the most sensitive wavelength for detecting a 1:1 complex. In Figure 4, the corresponding CD mixing curve demonstrates formation of a 1:1 complex and absence of a 1:2 complex. Wavelength dispersion curves from the UV spectra and UV derivative spectra (Figure 1 of the supplementary material; see paragraph at end of the paper regarding supplementary material) and mixing curves plotted from these (Figure 4) confirm the above conclusion.

Similar analyses for the pair $(r2NH_28MeA)_n$, $(rBrU)_n$ show that a double helix is formed but not a triple helix (Figure 5 and Figure 2 of the supplementary material).

These results confirm a stereochemical prediction that a triple helix cannot be formed. To form the hydrogen bonds required for attachment of a third strand, a T residue would have to assume the position indicated in Figure 6 (light lines), with the distance between the 8-methyl group and the 2-oxygen atom less than 3 Å. Since the sum of the van der Waals radii of these groups is 3.4 Å (Pauling, 1960), the contact is not allowed.

Thermal Transitions of Complexes with $(rU)_n$, $(rT)_n$, and $(rBrU)_n$. The double helix $(r2NH_28MeA)_n{\cdot}(rU)_n$ melts cooperatively, with a T_m of 21.5 °C and a transition breadth of

Table I: Spectroscopic Data

	Ultraviolet λ_{max} (nm)	ϵ_{max}	λ_{min} (nm)	ϵ_{min}
$(r2NH_28MeA)_n$[a]	207	23000	235	4960
	257	9660	270	7970
	280	8770		
$(rBrU)_n$[b]	279	8450	243	1820
$(r2NH_28MeA)_n\cdot(rBrU)_n$[c]	266	6150	239	3240
	277	6330	264	6130
$(r2NH_28MeA)_n\cdot(rT)_n$[d]	261	7740	238	3350
	CD λ_{max} (nm)	$\epsilon_L - \epsilon_R$	λ_{min} (nm)	$\epsilon_L - \epsilon_R$
$(r2NH_28MeA)_n$[a]	206	11.42	218	−5.94
	248	2.92	263	0.42
	280	2.73		
$(rBrU)_n$[b]	229	0.97	214	0.43
	298	0.46	266	−2.20
$(r2NH_28MeA)_n\cdot(rBrU)_n$[a]	218	7.90	204	−3.90
	275	3.27	257	−1.23
			296	−3.63
$(rT)_n$[d]	224	1.79	211	−1.04
	271	14.87	252	−5.17
$(r2NH_28MeA)_n\cdot(rT)_n$[d]	217	4.95	205	−2.99
	268	7.68	249	−3.01
			288	−5.86

[a] 0.1 M Na^+, 0.002 M sodium pyrophosphate, pH 8.0; 20 °C. [b] 0.1 M Na^+, 0.002 M sodium cacodylate, pH 6.1; 20 °C. [c] 0.1 M Na^+, 0.002 M sodium cacodylate, pH 6.8; 20 °C. [d] 0.1 M Na^+, 0.002 M sodium pyrophosphate, pH 8.0; 10 °C.

13 °C in 0.1 M Na^+ (Figure 1). T_m has a linear dependence on log [Na^+] with the slope d T_m/d log [Na^+] = 12.3 ± 0.7 °C (Figure 2). The transition breadth increases slightly with [Na^+], having values of 12, 13.8, 14.5, and 16.7 °C in 0.05, 0.3, 0.5, and 0.7 M Na^+, respectively.

The complex $(r2NH_28MeA)_n\cdot(rT)_n$ also melts cooperatively with a T_m of 39 °C in 0.1 M Na^+. In this case, however, the thermal profile is biphasic, particularly at low ionic strength (Figure 3 of the supplementary material). The first step represents the melting of the $(rT)_n$ self-structure. The existence of this less stable structure in the presence of an equivalent of complementary polymer is evidently due to a kinetic trap. At low ionic strength, intramolecular formation of the hairpin self-structure is much more rapid than intermolecular formation of the heteroduplex. Results of a salt dilution experiment are consistent with this interpretation. Five solutions were prepared in 0.1 M Na^+ and allowed to stand 4 days at 5 °C before dilution to lower ionic strength (0.012, 0.022, 0.032, 0.052, and 0.072 M Na^+). Comparison of melting curves of these diluted solutions with those of solutions prepared initially in low salt showed the following changes in percent $(rT)_n$ self-structure between the latter solutions and the former, respectively: 49 to 6 (0.012 M); 26 to 9 (0.022 M); 17 to 9 (0.032 M); 12 to 11 (0.052 M); 11 to 10 (0.072 M) (Figure 3 of the supplementary material). The residual ~10% of self-structure presumably results from a more rapid intramolecular than intermolecular reaction of $(rT)_n$ in a certain molecular weight range even at somewhat higher ionic strength. The slope of the salt dependence curve was calculated from solutions used in the salt dilution experiment to minimize the effect of overlapping transitions. The value of dT_m/d log [Na^+] is 13.2 ± 0.5 °C.

Melting curves of $(r2NH_28MeA)_n\cdot(rBr)_n$ are shown in Figure 1. The T_m is 56 °C in 0.1 M Na^+ and the transition breadth 10 °C. dT_m/d log [Na^+] is 7.9 ± 0.4 °C. The dependence of T_m on pH is negligible near pH 7. T_m values at various pHs (in parentheses) are 58.5 (6.03), 59.6 (6.39), 59.1 (7.04), 55.1 (7.55), and 50.0 °C (8.05). The decreases in T_m above ~pH 7.5 and below ~pH 6.5 result from entering the titration ranges of $(rBrU)_n$ and $(r2NH_28MeA)_n$, respectively.

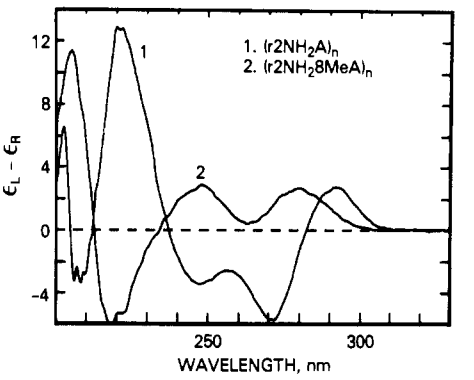

FIGURE 7: CD spectra of $(r2NH_2A)_n$ (curve 1) and $(r2NH_28MeA)_n$ (curve 2) both in 0.002 M sodium pyrophosphate, pH 8.0; [Na^+] = 0.1 M, 20 °C. Each curve is the average of nine spectra. CD spectra shown here and in succeeding figures were collected, processed, smoothed, and plotted with the LDACS 11/70 computer system.

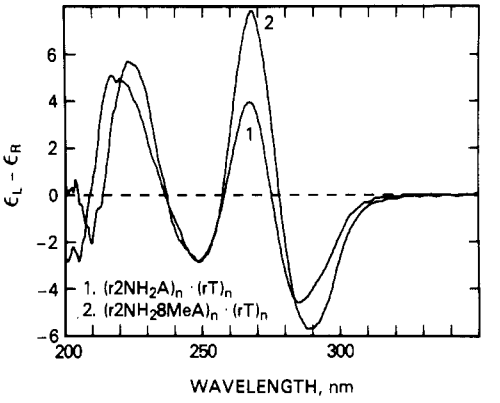

FIGURE 8: CD spectra of $(r2NH_2A)_n\cdot(rT)_n$ (curve 1; 20 °C) and of $(r2NH_28MeA)_n\cdot(rT)_n$ (curve 2; 10 °C). Conditions: 0.002 M sodium pyrophosphate, pH 8.0; [Na^+] = 0.1 M.

Electronic Spectra. The UV spectrum of $(r2NH_28MeA)_n$ has, like other $2NH_2A$ derivatives [cf. Howard et al. (1976) and Howard & Miles (1984)], three well-resolved bands at 280, 257, and 207 nm (Table I; Figure 4 of the supplementary material) assigned to B_{2u}, B_{1u}, and E_{1ua} transitions, respectively. As expected, the 8-Me residue has little effect on the $2NH_2A$ chromophore. The CD spectrum, however, has extrema at 280 (+2.7), 263 (minimum; +0.4), 248 (+2.9), 218 (−5.9), and 206 (+11.4) nm and differs in two significant respects from that of the electronically similar polymer $(r2NH_2A)_n$ (Figure 6; Table I). In $(r2NH_28MeA)_n$, the B_{2u} transition at 280 nm is not split, unlike that of $(r2NH_2A)_n$ (extrema at 291 and 273 nm). Extrema at higher energy occur at similar wavelengths but are inverted in sign (Figure 7). These marked differences in the homopolymers are contrasted below with the very similar spectra of the double helixes which these polymers form with $(rT)_n$.

The CD spectrum of $(r2NH_28MeA)_n\cdot(rT)_n$ has extrema at 288, 268, 249, 217, and 205 nm (Table I). Superimposed upon this in Figure 8 is the spectrum of the related helix $(r2NH_2A)_n\cdot(rT)_n$ having the same $2NH_2A$ and T chromophores [cf. Howard & Miles (1984)]. All of the bands have the same sign and are similar in wavelength, magnitude, and shape. The negative band at 288 nm (or 285 nm) is assigned to exciton splitting of the B_{2u} transition of $2NH_2A$. The two bands at 288 and 268 nm are conservative, with a mean value at the ultraviolet maximum. The second lobe of the split B_{2u} transition contributes to the band at 267 nm, as does, pre-

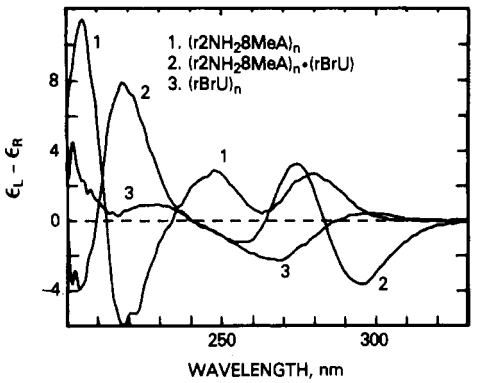

FIGURE 9: CD spectra of $(r2NH_28MeA)_n$ (curve 1), $(r2NH_28MeA)_n$·$(rBrU)_n$ (curve 2), and $(rBrU)_n$ (curve 3). Conditions: 20 °C; $[Na^+]$ = 0.1 M; 0.002 M sodium cacodylate, pH 6.8 (curves 2 and 3), or 0.002 M sodium pyrophosphate, pH 8.0 (curve 1).

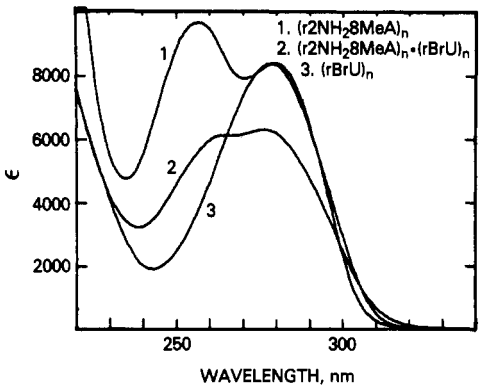

FIGURE 10: Ultraviolet spectra of $(r2NH_28MeA)_n$ (curve 1), $(r2NH_28MeA)_n$·$(rBrU)_n$ (curve 2), and $(rBrU)_n$ (curve 3). Maxima at 279 nm in the two homopolymers are assigned to B_{2u} transitions of the bases (see text). Conditions same as those in Table I.

sumably, the B_{2u} transition of T. Though overlap may obscure evidence of individual A and T contributions of the lower wavelength bands, these extrema can also be interpreted as exciton splittings of appropriate transitions [cf. Howard et al. (1976) and Mathelier et al. (1979)]. Independently of details of assignment, however, a major conclusion emerges from the CD spectra shown in Figures 7 and 8: the conformation of the purine residues is very similar in the two double helixes, but that of the single-stranded $(r2NH_28MeA)_n$ is quite different from either. The nature of this difference is discussed in a later section.

The CD spectrum of $(r2NH_28MeA)_n$·$(rBrU)_n$ has extrema at 296, 275, 257, 218, and 204 nm (Figure 9, Table I). We again assign the first two long-wavelength extrema to exciton splitting of the B_{2u} transition of 2-NH_2, but in this case, it appears that the B_{2u} transition of BrU is also split and contributes to the same pair. $(rBrU)_n$ has a UV maximum at 279 nm, coincident with that of $(r2NH_28MeA)_n$ and with that of the double helix formed by their interaction (Figure 10, Table I). Extrema of $(rBrU)_n$ occur at 291, 268, 236, and 209 nm at 6 °C and at 298, 266, 229, and 214 nm at 19 °C (Figure 5 of the supplementary material; Table I). The mean of the first two extrema of the homopolymer (19 °C) is 282 nm, and the mean of the corresponding pair in the complex is 285.5 nm. The observed displacements of the first pair of CD extrema from UV maxima in this complex are thus consistent with exciton splitting of the B_{2u} transitions of both $2NH_28MeA$ and 5BrU. As in the previous case, the presence of exciton splitting in the double helix but not in the purine single strand suggests a significantly different purine conformation in the two structures.

Table II: Thermal Properties of Helixes

	T_m $[Na^+]$		dT_m/d log $[Na^+]$	$\Delta H°_{calcd}$ (kcal/bp)[a]
	0.03 M	0.1 M		
(a) $(r2NH_28MeA)_n$·$(rU)_n$	15.3	21.3	12.3 ± 0.7	−8.9
(b) $(r2NH_2A)_n$·$(rU)_n$[b]	82.7	89.5	12.6 ± 0.4	−13.3
(c) $(r2NH_28MeA)_n$·$(rBrU)_n$	52.4	56.4	7.9 ± 0.4	−17.7
(d) $(r2NH_28MeA)_n$·$(rT)_n$	32.3	38.8	13.2 ± 0.5	−9.3
(e) $(r2NH_2A)_n$·$(rT)_n$[c]	93	100	12.8 ± 0.7	−13.8
(f) $(rA)_n$·$(rU)_n$[b]	46.3	57	17.1 ± 0.8	−7.9
(g) $(rA)_n$·$(rBrU)_n$	84 (3:1)	91 (3:1)		

[a] All $\Delta H°$ values calculated for 0.03 M Na^+. [b] Data from Muraoka et al. (1980). [c] Data from Howard & Miles (1984).

Discussion

A notable result of the present study is the sharp contrast in physical properties of the new polymer with those of $(r8MeA)_n$. The latter polymer forms no regular acid helix comparable to that of $(rA)_n$ but does form a regular helix at ambient temperature in neutral solution. It does not interact with any potentially complementary polynucleotide (Limn et al., 1983). $(r2NH_28MeA)_n$, in contrast, forms a regular acid helix but only a very unstable self-structure (T_m ~5 °C) in neutral solution. It readily forms double helixes, moreover, with $(rU)_n$ and $(rBrU)_n$ and $(rT)_n$. It is apparent that both the 2-NH_2 and 8-Me substitutions play important roles in determining the properties of the polymer containing them.

Previous work with dinucleoside monophosphates suggests that, while an 8-Me substituent shifts the glycosidic torsional equilibrium toward the syn range, it nevertheless does not exclude anti conformations (Uesugi et al., 1978; Ikehara et al., 1978). $(r8MeA)_n$ forms a single-stranded helix and appears to have both conformations present in the same chain (Limn et al., 1983). The failure of $(r8MeA)_n$ to react with $(rU)_n$ or $(rBrU)_n$ is presumably related to the presence of syn conformations in the chain, though both $(r8BrA)_n$ and Z DNA are known to form base-paired helical structures with purine bases in syn conformations. Govil et al. (1981) have suggested that failure of $(r8BrA)_n$ to react with $(rBrU)_n$ results from inability to bring into coincidence two helix axes which are quite differently disposed with respect to the BrA and BrU bases, and a similar explanation may apply to $(r8MeA)_n$.

Earlier studies have shown that 2-NH_2 substitution in $(rA)_n$ permits three A·U hydrogen bonds to be formed (Figure 6) and results in a T_m elevation of ~30 °C in the complex (Howard et al., 1966, 1976; Muraoka et al., 1980). One objective of the present study was to exploit the H-bonding and stabilizing potential of the 2-NH_2 group to drive the equilibrium in the direction of base pairing and helix formation. It is clear from the above results that this objective was achieved.

A number of factors affecting helix stability can be separated by careful comparison of pairs of complexes which differ only in the presence or absence of a chemical feature of interest [cf. Howard et al. (1969), Ikeda et al. (1970), and Howard & Miles (1984)]. In particular, algebraic sums of transition temperatures of selected pairs of helixes give ΔT_m values which characterize the energetic contribution of the chemical feature by which the two helixes differ. In the present case, relative contributions of the 8-Me and 2-NH_2 groups to helix stability can be estimated from the data in Table II. Thus, the T_m of $(r2NH_28MeA)_n$·$(rU)_n$ [(a) Table II] is 21.3 °C in 0.1 M Na^+, and that of $(r2NH_2A)_n$·$(rU)_n$ [(b) Table II] is 89.5 °C. The difference between these values is a measure of the de-

Table III: Dependence of T_m on $[Na^+]$

	range of $[Na^+]$	no. of observations	standard error of estimate, $\sigma_{x,y}$	equation
$(r2NH_28MeA)_n$[a]	0.03–0.1	4	0.6476	$T_m = -6.508 \log [Na^+] + 29.22$
$(r2NH_28MeA)_n$·$(rU)_n$	0.03–1.0	9	1.2918	$T_m = 12.268 \log [Na^+] + 33.60$
$(r2NH_28MeA)_n$·$(rT)_n$	0.012–0.072	5	0.3212	$T_m = 13.157 \log [Na^+] + 51.96$
$(r2NH_28MeA)_n$·$(rBrU)_n$	0.01–1.0	10	0.7301	$T_m = 7.944 \log [Na^+] + 64.31$

[a] At pH 6.20.

stabilizing effect of the 8-Me group toward double-helix formation, and the magnitude, 68 °C, indicates the effect is large. A similar value (61 °C) is obtained for the pair (e) – (d). The contribution of 5-Br substitution to the elevation of the helix T_m is 34 °C [Table II, (c) – (a) and (g) – (f)], in agreement with previous values [cf. Howard et al. (1969)]. While the T_m of poly($2NH_2A$)·poly(BrU) in 0.1 M Na^+ is too high for direct measurement, it can be estimated as the sum of 34 °C (ΔT_m for 5-Br) and 89 °C [(b), Table II] = 123 °C.

The foregoing results indicate that the 2-NH_2 group, contributing a T_m elevation of ~30 °C, does indeed provide enough stabilization to allow interaction within a measurable temperature range despite the much larger destabilizing effect of the 8-Me group. We suggest that both syn and anti conformations are present in the disordered $(r2NH_28MeA)_n$ chain and that formation of stable, 3 H-bond base pairs supplies the free energy to shift the equilibrium to the anti conformation. Possibly, a small population of anti bases in the chain provides nucleation points for growth of paired regions along the chain.

The salt dependence curves (Figure 2; Table III) have slopes of 12.3 ± 0.7 and 7.9 ± 0.4 °C for the $(rU)_n$ and $(rBrU)_n$ complexes, respectively. The former value is significantly lower than the slope of $(rA)_n$·$(rU)_n$ (17.1 °C) or $(rI)_n$·$(rC)_n$ (17.6 °C), and the value for the poly(BrU) complex appears to be the lowest yet reported for a double helix. We have found that complexes containing $2NH_2A$ such as $(r2NH_2A)_n$·$(rU)_n$ and $(r2NH_2A)$·$(rT)_n$ have low slopes (14.8 ± 0.7 and 12.8 ± 0.7 °C, respectively), but none have had values below 12 °C (Howard et al., 1976; Howard & Miles, 1984).

Slopes of salt dependence curves can be used to estimate enthalpies of dissociation of the complexes. Manning has applied his polyelectrolyte theory to obtain a relationship between ΔH and $dT_m/d \log [Na^+]$ (Manning, 1972, 1978). We have used this relationship in the form employed by Record et al. (1978) and found that it reproduced calorimetric enthalpies available in the literature with reasonable accuracy (Howard & Miles, 1984). The relation was also employed to estimate enthalpies for a number of helixes containing $2NH_2A$. The equation employed is

$$\frac{dT_m}{d \ln a_\pm} = \alpha \frac{RT_m^2}{\Delta H^\circ_{obsd}} \frac{\Delta\bar{\theta}_{M^+}}{2}$$

where ΔH°_{obsd} is the observed enthalpy of transition per mole of nucleotides, $a_\pm$ = the mean activity and is assumed $\simeq a$, $\alpha = 1 + d \ln \gamma_\pm / d \ln a_\pm \approx 0.95$ for 10^{-3} M $\leq [Na^+] \leq 10^{-1}$ M, $\gamma_\pm$ = the mean activity coefficient, and $\Delta\bar{\theta}_{M^+}$ = the number of counterions released per phosphate denatured. We use the value of $\Delta\theta = 0.32$, from Record et al. (1978), who obtained it by using ΔH° for AU → A + U reported by Krakauer & Sturtevant (1968).

The calculated value of ΔH for $(r2NH_28MeA)_n$·$(rU)_n$ in 0.03 M Na^+ is –8.9 kcal/base pair (bp) at T_m (15 °C). This result is higher than those of poly(I)·poly(C) and poly(I)·poly(BrC), for example, at 25 °C (–5.6 and –7.2 kcal/bp, respectively; Ross & Scruggs, 1969; Ross et al., 1971). The calculated enthalpy for $(r2NH_28MeA)_n$·$(rBrU)_n$ is much higher than any other value, measured or calculated: –18 kcal/bp at 56 °C. Since the 2-NH_2 group can increase ΔH by as much as –5 kcal/bp (Howard & Miles, 1984), and a 5-Br substituent can raise ΔH by –2 kcal/bp (Ross et al., 1971), a large enthalpy is anticipated. The magnitude of the increase, nevertheless, is striking. The high polarizability of the Br atom acting on the adjacent stacked bases is an important source of enthalpic increase (Howard et al., 1969; Ross et al., 1971) within the ordered BrU strand, and possibly between the strands as well. Other contributing factors include possible specific patterns of hydration and favorable stacking interactions of purine residues, as well as the third interbase hydrogen bond, discussed above.

Supplementary Material Available

Wavelength dispersion curves from the UV spectra and UV derivative spectra of the $(r2NH_28MeA)_n$, $(rT)_n$ pair (Figure 1) and the $(r2NH_28MeA)_n$, $(rBrU)_n$ pair (Figure 2), thermal profile of 1:1 mixtures of $(r2NH_28MeA)_n$ and $(rT)_n$ (Figure 3), UV spectra of $(r2NH_28MeA)_n$ and $(r2NH_2A)_n$ (Figure 4), and CD spectra of $(rBrU)_n$ and $(rT)_n$ (Figure 5) (5 pages). Ordering information is given on any current masthead page.

Registry No. $(r2NH_28MeA)_n$, 97374-44-2; $(rBrU)_n$, 27988-64-3; $(rT)_n$, 26700-96-9; $(r2NH_28MeA)_n$·$(rBrU)_n$, 97390-83-5; $(r2NH_28MeA)_n$·$(rT)_n$, 97374-45-3; $(r2NH_28MeA)_n$·$(rU)_n$, 97374-46-4; 2-amino-8-methyladenosine 5′-diphosphate, 97374-47-5.

References

Applequist, J., & Damle, V. (1966) *J. Am. Chem. Soc. 88*, 3895–3900.

Brahms, J. (1965) *J. Mol. Biol. 11*, 785–801.

Donohue, J., & Trueblood, K. N. (1960) *J. Mol. Biol. 2*, 363–371.

Drew, H. R., Takano, T., Tanaka, S., Itakura, K., & Dickerson, R. E. (1980) *Nature (London) 286*, 567–573.

Eisenberg, H., & Felsenfeld, G. (1967) *J. Mol. Biol. 30*, 17–37.

Govil, G., Fisk, C., Howard, F. B., & Miles, H. T. (1977) *Nucleic Acids Res. 4*, 2573–2592.

Govil, G., Fisk, C., Howard, F. B., & Miles, H. T. (1981) *Biopolymers 20*, 573–603.

Haschemeyer, A. E. V., & Rich, A. (1967) *J. Mol. Biol. 27*, 369–384.

Holcomb, D. N., & Tinoco, I. (1965) *Biopolymers 3*, 121–133.

Howard, F. B., & Miles, H. T. (1984) *Biochemistry 23*, 4219–4223.

Howard, F. B., Frazier, J., & Miles, H. T. (1966) *J. Biol. Chem. 241*, 4293–4295.

Howard, R. B., Frazier, J., & Miles, H. T. (1969) *J. Biol. Chem. 244*, 1291–1302.

Howard, F. B., Frazier, J., & Miles, H. T. (1975) *J. Biol. Chem. 250*, 3951–3959.

Howard, F. B., Frazier, J., & Miles, H. T. (1976) *Biochemistry 15*, 3783–3795.

Howard, F. B., Hattori, M., Frazier, J., & Miles, H. T. (1977) *Biochemistry 16*, 4637–4646.

Ikeda, K., Frazier, J., & Miles, H. T. (1970) *J. Mol. Biol. 54*, 59–84.

Ikehara, M., Tazawa, I., & Fukui, T. (1969) *Biochemistry 8*, 736–743.
Ikehara, M., Limn, W., & Fukui, T. (1977) *Chem. Pharm. Bull. 25*, 2702–2707.
Ikehara, M., Limn, W., & Uesugi, S. (1978) *J. Carbohydr., Nucleosides, Nucleotides 5*, 163–185.
Krakauer, H., & Sturtevant, J. M. (1968) *Biopolymers 6*, 491–512.
Limn, W., Uesugi, S., Ikehara, M., & Miles, H. T. (1983) *Biochemistry 22*, 4217–4222.
Manning, G. S. (1972) *Biopolymers 11*, 937–949.
Manning, G. S. (1978) *Q. Rev. Biophys. 11*, 179–246.
Mathelier, H. D., Howard, F. B., & Miles, H. T. (1979) *Biopolymers 18*, 709–722.
Maxam, A. M., & Gilbert, W. *Methods Enzymol. 65*, 499–560.
Michelson, A. M., Monny, C., & Kapuler, A. V. (1970) *Biochim. Biophys. Acta 217*, 7–15.
Moffat, J., & Khorana, H. G. (1961) *J. Am. Chem. Soc. 83*, 649–658.
Muraoka, M., Miles, H. T., & Howard, F. B. (1980) *Biochemistry 19*, 2429–2439.
Pauling, L. *The Nature of the Chemical Bond*, p 260, Cornell University Press, Ithaca, NY.
Powell, J. I., Fico, R., Jennings, W. H., O'Bryan, E. R., & Schultz, A. R. (1980) *Proc. IEEE Comput. Soc., Int. Conf., 21st*, 185–190.
Ross, P. D., & Scruggs, R. L. (1969) *J. Mol. Biol. 45*, 567–569.
Ross, P. D., Scruggs, R. L., Howard, F. B., & Miles, H. T. (1971) *J. Mol. Biol. 61*, 727–733.
Record, M. T., Anderson, C. F., & Lohman, T. M. (1978) *Q. Rev. Biophys. 11*, 103–178.
Sakore, T. D., & Sobell, H. M. (1969) *J. Mol. Biol. 43*, 77–87.
Silverton, J. V., Limn, W., & Miles, H. T. (1982) *J. Am. Chem. Soc. 104*, 1081–1087.
Sundaralingam, M. (1973) *Jerusalem Symp. Quantum Chem. Biochem. 5*, 417–455.
Tavale, S. S., & Sobell, H. M. (1970) *J. Mol. Biol. 48*, 109–123.
Wang, A. H. J., Quigley, G. J., Kolpak, F. J., Crawford, J. L., van Boom, J. H., van der Marel, G., & Rich, A. (1979) *Nature (London) 282*, 680–686.
Zimmerman, S. B. (1982) *Annu. Rev. Biochem. 51*, 395–427.

Nonenzymic Adenosine 5′-Diphosphate Ribosylation of Poly(adenosine diphosphate ribose)†

Miyoko Ikejima* and D. Michael Gill
Department of Molecular Biology and Microbiology, Tufts University School of Medicine, Boston, Massachusetts 02111
Received January 4, 1985

ABSTRACT: Poly(adenosine 5′-diphosphate ribose) [poly(ADP-ribose)] is spontaneously ADP-ribosylated when it is incubated with nicotinamide adenine dinucleotide, especially in 0.5 M NaCl and at an alkaline pH. The ADP-ribose residues are monomeric and are attached to the middle of polymer chains. The linkage is similar to, and may be identical with, that of the branch points that are created in cells. RNA is also spontaneously ADP-ribosylated, but not DNA.

Poly(adenosine 5′-diphosphate ribose) [poly(ADP-ribose)] is a nuclear macromolecule that is synthesized at DNA breaks and may play some role in their repair (Juarez-Salinas et al., 1979; Benjamin & Gill, 1980a; Berger et al., 1980; Durkacz et al., 1980; Shall, 1983; Ikejima et al., 1983). It is rapidly degraded in situ, and the newly synthesized material has a complete range of sizes up to at least several hundred residues (Tanaka et al., 1978; Benjamin & Gill, 1980a,b; Ikejima et al., 1983). For the most part, the polymer consists of ADP-ribose residues joined in series by 1″→2′ glycosidic bonds between ribose residues, but there are branches involving 1‴→2″ ribose→ribose bonds approximately every 50–100 residues (Miwa et al., 1979; Juarez-Salinas et al., 1982; Kanai et al., 1982; Sugimura & Miwa, 1982). The structure of a branch point is shown in Figure 1A. After digestion by snake venom phosphodiesterase, backbone residues yield phosphoribosyl-AMP (PR-AMP)[1] while the branch points yield di-(phosphoribosyl)-AMP [(PR)2-AMP] (Figure 1).

We have found that pure poly(ADP-ribose) itself becomes radioactive when it is incubated with radioactive NAD. The product consists of radioactive ADP-ribose residues attached to internal sites along poly(ADP-ribose) chains. By several criteria, these attachments are indistinguishable from the poly(ADP-ribose) branch points formed in cellular environments. Although the rate is slow under the conditions we have used, the reaction may illuminate the mechanism whereby poly(ADP-ribose) polymerase introduces branch points, and we discuss whether the natural branching mechanism may include a nonenzymic step.

Experimental Procedures

Poly(ADP-ribose) composed of chains of 10–30 ADP-ribose residues was a gift from Dr. Masanao Miwa, National Cancer Center Research Institute, Tokyo, Japan. After digestion with phosphodiesterase, nucleotide analysis using high-performance

† This work was supported by Grant GM28482 from the National Institutes of Health.

[1] Abbreviations: PR-AMP, 2′-(5″-phosphoribosyl)adenosine 5′-phosphate, 2′-ribosyladenosine 5′,5″-bis(phosphate), or *O*-α-D-ribofuranosyl(1″→2′)adenosine 5′,5″-bis(phosphate); (PR)2-AMP, 2′-[2″-(5‴-phosphoribosyl)-5″-phosphoribosyl]adenosine 5′-phosphate, 2′-[2″-(1‴-ribosyl)-1″-ribosyl]adenosine 5′,5″,5‴-tris(phosphate), or *O*-α-D-ribofuranosyl(1‴→2″)-*O*-α-D-ribofuranosyl(1″→2′)adenosine 5′,5″,5‴-tris(phosphate).

0006-2960/85/0424-5039$01.50/0